Original Research

Hypoxia Triggers Osteochondrogenic Differentiation of Vascular Smooth Muscle Cells in an HIF-1 (Hypoxia-Inducible Factor 1)–Dependent and Reactive Oxygen Species–Dependent Manner

Enikő Balogh,* Andrea Tóth,* Gábor Méhes, György Trencsényi, György Paragh, Viktória Jeney

Objective—Vascular calcification is associated with high risk of cardiovascular events and mortality. Osteochondrogenic differentiation of vascular smooth muscle cells (VSMCs) is the major cellular mechanism underlying vascular calcification. Because tissue hypoxia is a common denominator in vascular calcification, we investigated whether hypoxia per se triggers osteochondrogenic differentiation of VSMCs.

Approach and Results—We studied osteochondrogenic differentiation of human aorta VSMCs cultured under normoxic (21% O_2) and hypoxic (5% O_2) conditions. Hypoxia increased protein expression of HIF (hypoxia-inducible factor)-1α and its target genes GLUT1 (glucose transporter 1) and VEGFA (vascular endothelial growth factor A) and induced mRNA and protein expressions of osteochondrogenic markers, that is, RUNX2 (runt-related transcription factor 2), SOX9 (Sry-related HMG box-9), OCN (osteocalcin) and ALP (alkaline phosphatase), and induced a time-dependent calcification of the extracellular matrix of VSMCs. HIF-1 inhibition by chetomin abrogated the effect of hypoxia on osteochondrogenic markers and abolished extracellular matrix calcification. Hypoxia triggered the production of reactive oxygen species, which was inhibited by chetomin. Scavenging reactive oxygen species by *N*-acetyl cysteine attenuated hypoxia-mediated upregulation of HIF-1α, RUNX2, and OCN protein expressions and inhibited extracellular matrix calcification, which effect was mimicked by a specific hydrogen peroxide scavenger sodium pyruvate and a mitochondrial reactive oxygen species inhibitor rotenone. Ex vivo culture of mice aorta under hypoxic conditions triggered calcification which was inhibited by chetomin and *N*-acetyl cysteine. In vivo hypoxia exposure (10% O_2) increased RUNX2 mRNA levels in mice lung and the aorta.

Conclusions—Hypoxia contributes to vascular calcification through the induction of osteochondrogenic differentiation of VSMCs in an HIF-1–dependent and mitochondria-derived reactive oxygen species–dependent manner. (*Arterioscler Thromb Vasc Biol*. 2019;39:00-00. DOI: 10.1161/ATVBAHA.119.312509.)

Key Words: hypoxia ◼ hypoxia-inducible factor 1 ◼ mitochondria ◼ reactive oxygen species ◼ vascular calcification

Vascular calcification (VC) increases progressively during aging and associated with higher risks for any cardiovascular event and mortality.[1–4] Diverse pathologies including chronic kidney disease, diabetes mellitus, atherosclerosis, as well as chronic respiratory diseases are associated with accelerated calcification.[5–8]

Osteochondrogenic differentiation of vascular smooth muscle cells (VSMCs) is considered to be the key event in VC.[9,10] Upon osteochondrogenic differentiation, VSMCs upregulate master transcription factors of osteogenesis and chondrogenesis, such as RUNX2 (runt-related transcription factor 2) and SOX9 (Sry-related HMG box-9); parallel with this process, they lose VSMC lineage markers such as smooth muscle actin α-2.[9–13] RUNX2, SOX9, and their target genes

such as ALP (alkaline phosphatase) and OCN (osteocalcin) are found to be upregulated in calcifying vascular tissues.[9–13] Several inducers and inhibitors of such transdifferentiation have been identified to date.[14–17]

Accumulating evidence suggests a link between hypoxia and accelerated calcification. For example, arterial calcification is increased in patients with asthma, chronic obstructive pulmonary disease, and obstructive sleep apnea,[6–8] but whether hypoxia plays a contributory role in triggering arterial calcification in these conditions has not been addressed.

HIF-1 (hypoxia-inducible factor 1) pathway is the master regulator of cellular and systemic homeostatic response to hypoxia. The HIF-1 pathway is regulated by the oxygen-sensitive α subunit (HIF-1α) that is stabilized upon hypoxia.[18]

Nonstandard Abbreviations and Acronyms	
ALP	alkaline phosphatase
BRD4	bromodomain protein 4
DPBS	Dulbecco's PBS
ECM	extracellular matrix
GLUT1	glucose transporter protein type 1
HIF-1	hypoxia-inducible factor 1
NAC	*N*-acetyl cysteine
OCN	osteocalcin
OD	optical density
ROS	reactive oxygen species
RUNX2	runt-related transcription factor 2
SOX9	Sry-related HMG box-9
SP	sodium pyruvate
VC	vascular calcification
VEGFA	vascular endothelial growth factor A
VSMC	vascular smooth muscle cell

Some studies associated HIF-1α levels and VC. For example, a positive correlation between plasma HIF-1α levels and arterial calcification has been shown in patients with type 2 diabetes mellitus.[19] In addition, a study revealed that HIF-1α colocalizes with neoangiogenesis and areas of calcification in stenotic valves.[20]

Recently, a direct role of HIF-1 activation has been shown in phosphate-induced VSMC calcification that could be relevant in mineral imbalance-induced calcification in patients with chronic kidney disease.[21] Moreover, pulmonary arterial hypertension was found to be associated with increased pulmonary arterial calcification and elevated expression of RUNX2 in the lungs of patients with pulmonary arterial hypertension.[22] These works proposed that sustained RUNX2 expression promotes HIF-1α activation and that RUNX2/HIF-1α axis triggers proliferative and osteogenic phenotype switch of VSMCs.[21,22]

Hypoxia triggers adaptation mechanisms, including but not limited to angiogenesis, vascular reactivity and remodeling and metabolic alterations such as upregulation of glucose uptake and glycolysis to foster survival in a low oxygen condition.[23] As part of the hypoxic response, cells reduce oxygen consumption of mitochondria through the upregulation of pyruvate dehydrogenase kinase 1 that leads to inactivation of pyruvate dehydrogenase which prevents the conversion of pyruvate to acetyl-CoA and thus attenuates the entry of pyruvate to the mitochondrial Krebs cycle.[24]

It is generally accepted that intracellular reactive oxygen species (ROS) levels also change during hypoxia, but the direction of this change and the origin of ROS (mitochondrial or NADPH oxidase) remained controversial.[25] Because ROS production requires oxygen one might assume that ROS production is attenuated in hypoxia which idea is supported by several studies.[25] On the other hand, accumulating evidence suggests that hypoxia-mediated partial inhibition of the mitochondrial electron transport chain is associated with increased mitochondrial ROS production.[26–30] Recent evidence suggests that upon hypoxia mitochondria-derived elevated ROS production stabilizes HIF-1α; and therefore, elevated ROS production plays a critical role in hypoxia-driven cellular responses.[29–31]

Unfettered ROS production has been implicated in cardiovascular pathophysiology including VC.[32] Elevated ROS formation was detected in animal models of VC and in human sclerotic and stenotic aortic valves.[33] Vascular cells expressing osteogenic markers were identified as a source of excess ROS, and in vitro studies revealed that ROS production is enhanced during osteogenic differentiation of VSMCs.[33] A recent study showed that inhibition of mitochondrial ROS generation attenuates phosphate-mediated osteogenic differentiation of VSMCs, suggesting a causative role of ROS in VC.[34] Because hypoxia is a common feature in diverse pathologies when cardiovascular calcification occurs, here we investigated the role of hypoxia, HIF-1 activation, and ROS formation in osteochondrogenic differentiation of human aortic SMCs.

Materials and Methods

The article adheres to the implementation of the Transparency and Openness Promotion Guidelines. The data that support the findings of this study are available from the corresponding author upon request.

Materials

Unless specified otherwise, reagents were from Sigma-Aldrich Co (St Louis, MO).

Mice

All experiments were performed in compliance with institutional (Institutional Ethics Committee, University of Debrecen) and national guidelines. Twenty-four C57BL/6 mice (8–10 weeks old, male and female, sex matched) were randomly divided into 4 groups. Mice were housed in cages with standard bedding and unlimited access to food and water placed into transparent gas-tight acrylic chambers. The hypoxia group obtained a premade gas mixture of 10% O_2 and 90% of N_2 (Messer Group GmbH, Bad Soden, Germany). The normoxia group obtained a premade gas mixture of 21% O_2 and 79% of N_2 (Messer Group GmbH). The total gas flow through the chamber was adjusted to 5 to 10 L/min. Temperature was maintained at 24°C to 26°C, and a standard light-dark cycle of ≈12-hour light exposure was used. At the indicated time of hypoxia exposure (12, 24, and 48 hours), mice were sacrificed with CO_2 inhalation and perfused with 5 mL of ice-cold Dulbecco's PBS (DPBS; D8537; Sigma). Aorta and lung samples were collected, snap-frozen in liquid N_2, and kept at −80°C until analysis.

Cell Culture and Reagents

Human aorta VSMCs (354-05; Cell Applications Inc, San Diego, CA) were maintained in DMEM (D6171; Sigma) supplemented with 10% FBS (F2442; Sigma), antibiotic-antimycotic solution (A5955; Sigma), and L-glutamine (G7513; Sigma). Cells were maintained at 37°C in a humidified atmosphere containing 5% CO_2. Cells were grown to confluence and used from passages 5 to 8. Experiments were performed on 2 cell lines derived from different donors. In some experiments, we cultured VSMCs in osteogenic medium that was obtained by supplementing the growth medium with inorganic phosphate (NaH_2PO_4-Na_2HPO_4, pH 7.4, 2.5 mmol/L; S5011 and S5136; Sigma) and $CaCl_2$ (0.6 mmol/L; C8106; Sigma).

Hypoxic Treatment

Hypoxic condition was obtained by placing the cells into a modular incubator chamber (Billups-Rothenberg Inc, Del Mar, CA), which was connected to a gas bottle containing a mixture of 5% O_2, 5%

CO_2, and 94% of N_2 (Messer Group GmbH). A continuous slow flow (0.1 L/min) was applied throughout the experiment. To obtain normoxia, we used a gas mixture of 21% O_2, 5% CO_2, and 74% of N_2. In some experiments, we used hypoxia mimetic drugs $CoCl_2$ (CC, 200 µmol/L; 60818; Sigma), desferrioxamine (20 µmol/L; D9533; Sigma), 2, 2′-bipyridyl (100 µmol/L; D216305; Sigma), or the HIF-1 inhibitor chetomin (6 nmol/L; C9623; Sigma).

Alizarin Red Staining and Quantification

Alizarin red staining was performed as described previously.[35] In brief, after washing with DPBS, the cells were fixed in 4% paraformaldehyde (16005; Sigma) and rinsed with deionized water thoroughly. Cells were stained with Alizarin Red S (A5533; Sigma) solution (2%, pH 4.2) for 20 minutes at room temperature. Excessive dye was removed by several washes in deionized water. To quantify alizarin red staining in 96-well plates, we added 100 µL of hexadecylpyridinium chloride (C9002; Sigma) solution (100 mmol/L) to the wells and measured optical density (OD) with a spectrophotometer (Hitachi U-2800A) at 560 nm using hexadecylpyridinium chloride solution as blank.

Determination of Cell Viability

Cell viability was determined by the 3-[4, 5-Dimethylthiazol-2-yl]-2,5-diphenyl-tetrazolium bromide assay as previously described.[36] In brief, cells were cultured and treated in 96-well plates for the indicated time. Then cells were washed with DPBS, and 100 µL of 3-[4, 5-Dimethylthiazol-2-yl]-2,5-diphenyl-tetrazolium bromide (0.5 mg/mL; M2128; Sigma) solution in DPBS was added. After a 4-hour incubation, the 3-[4, 5-Dimethylthiazol-2-yl]-2,5-diphenyl-tetrazolium bromide solution was removed, formazan crystals were dissolved in 100 µL of DMSO (D8779; Sigma), and OD was measured with a spectrophotometer (Hitachi U-2800A) at 570 nm using DMSO as blank. Viability of nontreated cells at day 0 was considered as 100%, whereas viability of cells treated with 1% Triton X-100 (X100; Sigma) was considered as 0%. We used the following equation to calculate viability of samples: viability of sample=[$OD570_{sample}$ / ($OD570_{Day0\ Ctrl} - OD570_{Triton\ x-100}$)]×100.

ALP Activity Assay

Cells grown in 96-well plates were washed with DPBS twice, solubilized with 1% Triton X-100 in 0.9% NaCl (S7653; Sigma) and assayed for ALP activity. In brief, 130 µL of Alkaline Phosphatase Yellow Liquid Substrate (P7998; Sigma) was combined with 50 µg of protein samples, incubated at 37°C for 30 min, and then the kinetics of p-nitrophenol formation was followed for 30 minutes at 405 nm. Maximum slope of the kinetic curves was used for calculation.

Quantification of Ca Deposition

Cells grown on 96-well plates were washed twice with DPBS and decalcified with HCl (30721; Sigma; 0.6 mol/L) for 30 minutes at room temperature. Ca content of the HCl supernatants was determined by QuantiChrom Calcium Assay Kit (DICA-500; Gentaur, Kampenhout, Belgium) as previously described.[37] Following decalcification, cells were washed twice with DPBS and solubilized with a solution of NaOH (S8045; Sigma; 0.1 mol/L) and sodium dodecyl sulfate (20760; Sigma; 0.1%), and protein content of samples were measured with BCA protein assay kit (23225; Pierce Biotechnology, Rockford, IL). Ca content of the cells was normalized to protein content and expressed as µg/mg protein.

Quantitative Reverse Transcription Polymerase Chain Reaction

RNA was isolated from cells using Trizol (CS502, RNA-STAT60; Tel-Test Inc, Friendswood, TX) according to the manufacturer's protocol. Two micrograms of RNA was reverse transcribed to cDNA with High-Capacity cDNA Reverse Transcription Kit (4368813; Applied Biosystems, Waltham, MA). Quantitative real-time polymerase chain reaction was performed using iTaq Universal Probes Supermix (172–5134; BioRad Laboratories, Hercules, CA) and predesigned primers and probes (TaqMan Gene Expression Assays) to detect *VEGFA* (Hs.00900055), *GLUT1* (Hs.00892681), *RUNX2* (Hs.535845), *SOX9* (Hs.1001343), *MSX2* (Hs.00741177), *ALP* (Hs.00768162), *OCN* (Hs.01587814), *GAPDH* (Hs.02758991), and *Cyclophilin A* (Hs04194521). Relative mRNA expressions were calculated with the ΔΔCt method using *GAPDH* or *CyPA* as internal control.

Western Blot Analysis

We evaluated HIF-1α, Glut-1, RUNX2, SOX9, and ALP protein expressions in whole cell lysates. Proteins (20 µg/lane) were resolved on 10% SDS-PAGE, then blotted onto a nitrocellulose membrane (Amersham Proton 1060003; GE Healthcare, Chicago, IL). Western Blotting was performed with the use of an anti–HIF-1α antibody (GTX30647; GeneTex, Irvine, CA) at a 1 µg/mL concentration, anti–Glut-1 antibody (GTX15309; GeneTex) at a 0.5 µg/mL concentration, anti-RUNX2 antibody (20700-1-AP; Proteintech, Rosemont, IL) at 0.2 µg/mL concentration, anti-SOX9 antibody (ab184547; Abcam, Cambridge, United Kingdom) at 1 µg/mL concentration, and anti-ALP antibody (sc-30203; Santa Cruz Biotechnology, Inc, Dallas, TX) at 1 µg/mL concentration. After the binding of the primary antibodies, membranes were incubated with Amersham ECL Rabbit IgG, HRP-linked whole Ab (NA-934; GE Healthcare) at 0.5 µg/mL concentration. Antigen-antibody complexes were visualized with Amersham ECL Western Blotting Detection Reagent (RPN2109; GE Healthcare). After detection, the membranes were stripped and reprobed for β-actin with the use of an anti–β-actin antibody (sc-47778; Santa Cruz Biotechnology, Inc) at a concentration of 0.5 µg/mL. Results were quantified by using Alpha DigiDoc RT (Alpha Innotech, San Leandro, CA).

Quantification of OCN

For OCN detection, the extracellular matrix (ECM) of cells grown on 6-well plates was dissolved in 100 µL of EDTA (E6758; Sigma; 0.5 mol/L, pH 6.9). Concentration of OCN was quantified by an ELISA (BMS2020INST; eBioscience, San Diego, CA) using 25 µL of the EDTA-solubilized ECM samples.

Intracellular ROS Measurement

ROS production was monitored by using the 5-(and-6)-chloromethyl-2′,7′-dichlorodihydro-fluorescein di-acetate, acetyl ester assay (C6827; Life Technologies, Carlsbad, CA) as previously described.[38] After a 4-hour pretreatment, cells were washed with DPBS and loaded with 5-(and-6)-chloromethyl-2′,7′-dichlorodihydro-fluorescein di-acetate, acetyl ester (10 µmol/L, 30 minutes, in the dark). Cells were washed thoroughly with DPBS, and fluorescence intensity was measured in every 30 minutes for 4 hours applying 488 nm excitation and 533 nm emission wavelengths. In some experiments, we applied ROS inhibitors during the hypoxia treatment, *N*-acetyl cysteine (NAC, 1 mmol/L; A9165; Sigma), Mn(III)-tetrakis (4-benzoic acid) porphyrin chloride (50 µmol/L; sc-221954; Santa Cruz Biotechnology, Inc), sodium pyruvate (SP, 5 mmol/L; P5280; Sigma), GKT137831 (GKT, 20 µmol/L; HY-12298; MedChem Express, Sollentuna, Sweden), and rotenone (5 µmol/L; R8875; Sigma).

Aorta Organ Culture Model and Quantification of Ca

C57BL/6 mice (N=35 in total, N=5 per group) were sacrificed with CO_2 inhalation and perfused with 5 mL of ice-cold DPBS. Entire aortas were harvested and cleaned using a dissecting microscope under aseptic conditions. Aortas were maintained in DMEM (D6171; Sigma) supplemented with 10% FBS (F2442; Sigma), antibiotic-antimycotic solution (A5955; Sigma), and L-glutamine (G7513; Sigma) under hypoxic (5% O_2) or normoxic conditions for 6 days. As positive control, we used osteogenic medium that was obtained by supplementing the basal culture medium with inorganic phosphate

(NaH$_2$PO$_4$-Na$_2$HPO$_4$, pH 7.4, 2.5 mmol/L) as previously described.[39] In some experiments, we applied NAC (5 mmol/L) and chetomin (6 nmol/L) during the hypoxia treatment. The medium was replaced in every other day. After 6 days of treatment, aortas were opened longitudinally and decalcified with 50 µL of HCl (30721; Sigma; 0.6 mol/L) for 30 minutes at room temperature. Ca content of the HCl supernatants was determined by QuantiChrom Calcium Assay Kit (DICA-500; Gentaur, Kampenhout, Belgium) and normalized to the wet weight of the aortas.

Statistical Analysis

Results are expressed as mean±SD. At least 3 independent experiments were performed for all in vitro studies. Statistical analyses were performed with GraphPad Prism software (version 8.01, San Diego, CA). Shapiro-Wilk test was performed to assess normality of distribution. All data passed normality and equal variance tests; therefore, parametric tests were used to determine *P* values. Statistically significant differences between 2 groups were assessed using a 2-tailed Student *t* test. Comparisons between >2 groups were performed by 1-way ANOVA followed by Tukey multiple comparisons test. To compare each of a number of treatment groups with a single control group, we performed 1-way ANOVA followed by Dunnett post hoc test. Because of low mice number/group, data from male and female mice were analyzed together in the ex vivo and in vivo experiments. A value of *P* <0.05 was considered significant.

Results

Hypoxia Induces Osteochondrogenic Differentiation and ECM Mineralization of VSMCs

To investigate whether hypoxia plays a role in osteochondrogenic reprogramming of human VSMCs first we investigated whether hypoxia (5% O$_2$) or the hypoxia mimetics CoCl$_2$ (200 µmol/L), desferrioxamine (20 µmol/L) and 2,2′-bipyridyl (100 µmol/L) trigger stabilization of HIF-1α in VSMCs. After 12 hours of treatment, we evaluated protein expression of HIF-1α from whole cell lysate (Figure 1A). We found that hypoxia as well as all the hypoxia mimetics increased HIF-1α levels markedly (≈5- to 8-fold) in VSMCs. Because GLUT1 (glucose transporter 1) and VEGFA (vascular endothelial growth factor A) are regulated by the HIF-1 pathway next we evaluated protein expressions of GLUT1 and VEGFA. Hypoxia and hypoxia mimetics increased GLUT1 expression (12 hours) and VEGFA secretion (48 hours) in VSMCs (Figure 1A and 1B). Parallel with these changes, hypoxia (5% O$_2$, 6 hours) caused a 2- to 3-fold elevation of mRNAs encoding osteochondrogenic transcription factors, that is, *RUNX2*, *SOX9*, and *Msh Homeobox 2* (*MSX2*; Figure 1C). Moreover, we found that mRNA levels of *OCN* and *ALP*, genes under the control of the osteochondrogenic transcription factors, were also elevated in VSMCs exposed to hypoxia (1.52±0.04 fold and 1.8±0.08 fold increases over normoxia controls, respectively; Figure 1C).

Next, we evaluated protein expressions of RUNX2, SOX9, and ALP in VSMCs exposed to normoxia or hypoxia for 12 hours, 3 days, and 6 days. Compared with normoxia controls, expressions of RUNX2 and SOX9 were elevated at 12 hours and 6 days (Figure 1D). Protein expression as well as enzyme activity of ALP was increased after 6 days of hypoxia exposure (Figure 1D and 1E). Next, we have measured the level of OCN, a major noncollagenous protein in mineralized bone, in the ECM of VSMCs in every 5 days for 20

days. Concentration of OCN was low and did not change in VSMCs under normoxia (Figure 1F). In contrast, hypoxia triggered a time-dependent elevation of OCN levels in the ECM (days 15 and 20).

To study whether the observed hypoxia-induced lineage reprogramming of VSMCs leads to ECM calcification, we exposed VSMCs to hypoxia for 10 days and measured Ca deposition in the ECM. As a positive control, we used osteogenic medium that was supplemented with phosphate (2.5 mmol/L) and Ca (0.6 mmol/L), that is a well-established inducer of ECM calcification in VSMCs. Hypoxia triggered time-dependent Ca accumulation in the ECM although the calcification was delayed and weaker compared with phosphate-mediated Ca deposition (Figure 2A). This result was confirmed by alizarin red staining, which showed weak positivity following a 10-day hypoxia exposure (Figure 2B). These results suggest that hypoxia per se acts as an osteogenic factor in VC in vitro.

Calcification of VSMCs has been associated with apoptotic cell death especially in high phosphate and calcium conditions[10]; therefore, next we investigated whether cell death could play a role in hypoxia-induced ECM calcification in VSMCs. We exposed VSMCs to hypoxia or osteogenic medium and measured cell viability after 10 days of treatment. None of the treatments influenced cell viability that remained higher than 90% after 10 days of treatment when compared with cell viability determined on day 0 (Figure 2C).

Hypoxia Triggers Osteochondrogenic Differentiation of VSMC Through HIF-1

In general, hypoxia-induced cellular responses are mediated via HIF-1. To test whether HIF-1 activation is involved in hypoxia-mediated osteochondrogenic differentiation of VSMCs we applied chetomin, a well-characterized and selective inhibitor of HIF-1 transcriptional activity. First, we checked the efficiency of chetomin in inhibiting HIF-1 activity by evaluating mRNA levels and protein expressions of VEGFA and GLUT1. In response to hypoxia (5% O$_2$, 6 hours) VSMCs upregulated both *VEGFA* and *GLUT1* transcriptions which responses were completely abolished in the presence of chetomin (Figure 3A). Then we evaluated the level of VEGFA in supernatant of VSMCs cultured under hypoxic conditions in the presence or absence of chetomin for 48 hours (Figure 3B). Chetomin inhibited hypoxia-mediated upregulation of VEGFA formation (Figure 3B). In addition, we found that chetomin attenuated the increase in GLUT1 protein expression triggered by hypoxia (5% O$_2$, 12 hours; Figure 3C).

Next we investigated the effect of chetomin on hypoxia-induced upregulation of osteochondrogenic markers. In the presence of chetomin hypoxia-induced increase in *RUNX2*, *SOX9*, *MSX*2 *OCN*, and *ALP*, mRNA levels were abrogated (Figure 3D). Chetomin abolished upregulation of RUNX2 protein expression induced by hypoxia (5% O$_2$, 12 hours; Figure 3E). In addition, chetomin inhibited hypoxia-mediated increase in OCN in the ECM (day 15; Figure 3F) and ECM calcification (day 10; Figure 3G). These results suggest that HIF-1 activity plays a role in hypoxia-mediated osteochondrogenic differentiation and ECM calcification of VSMCs.
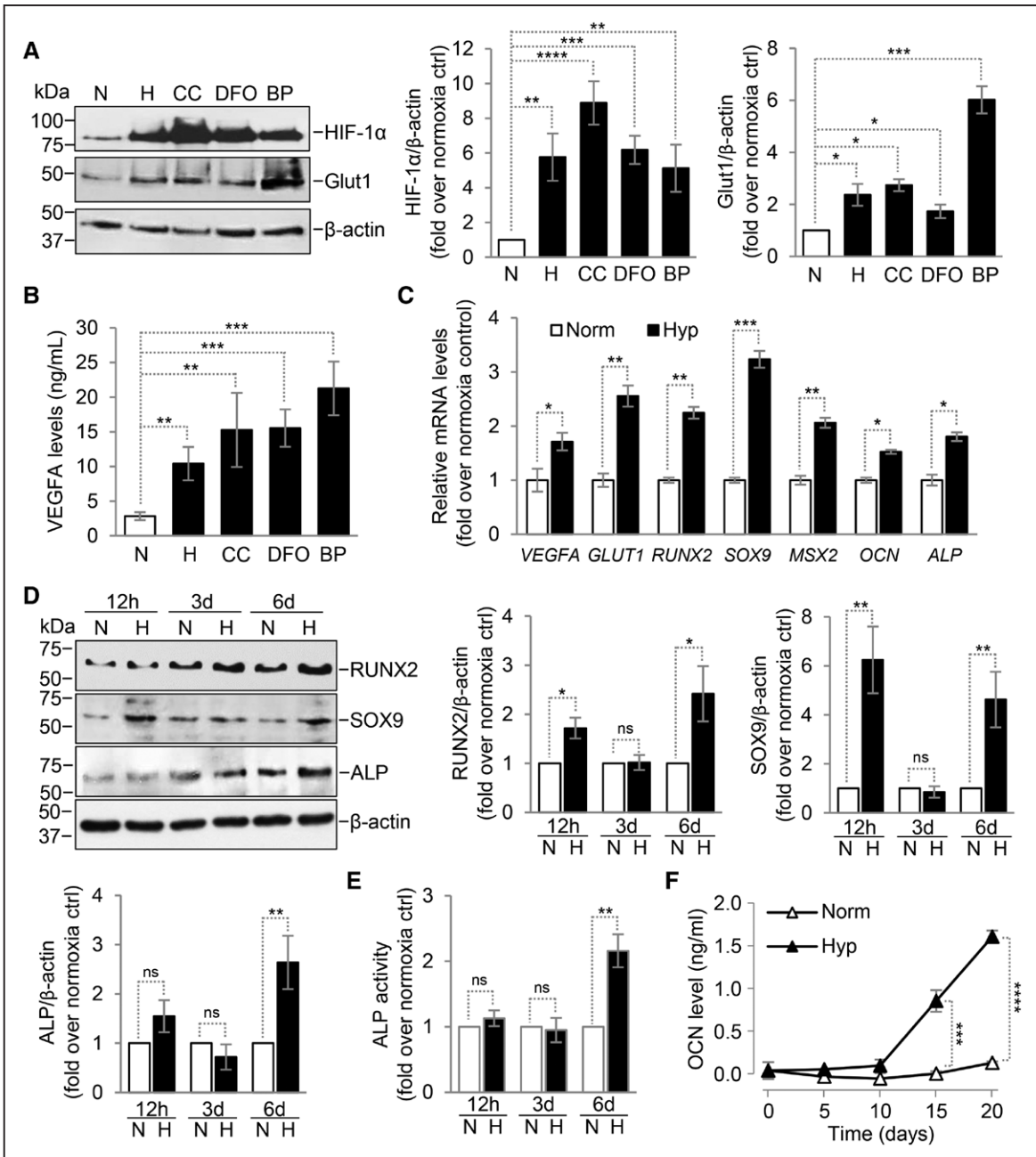
Figure 1. Hypoxia induces osteochondrogenic differentiation of vascular smooth muscle cells (VSMCs). Confluent VSMCs (passage 5–8) were maintained under normoxic (N, 21% O_2) or hypoxic (H, 5% O_2) conditions or exposed to the hypoxia mimetic drugs $CoCl_2$ (CC, 200 µmol/L), desferrioxamine (DFO, 20 µmol/L), bipyridyl (BP, 100 µmol/L). **A**, HIF (hypoxia-inducible factor)-1α, Glut-1 (glucose transporter 1), and β-actin protein expressions detected by Western Blot from whole cell lysate (12 h). Representative Western blots from 3 independent experiments. Densitometry analysis (mean±SD) of 3 independent experiments. **B**, VEGFA (vascular endothelial growth factor A) levels (48 h, mean±SD) were determined from cellular supernatant by ELISA in triplicates from 4 independent experiments. **C**, Relative mRNA expressions (6 h, mean±SD) of *VEGFA*, *GLUT1*, *RUNX2*, *SOX9*, *MSX2*, *OCN*, *ALP* normalized to *GAPDH* from 3 independent experiments performed in triplicates. **D**, RUNX2 (runt-related transcription factor 2), SOX9 (Sry-related HMG box-9), ALP (alkaline phosphatase), and β-actin protein expressions detected by Western Blot from whole cell lysate (12 h, 3 d, 6 d). Representative Western blots from 3 independent experiments. Densitometry analysis (mean±SD) of 3 independent experiments. **E**, Alkaline phosphatase activity (mean±SD) of VSMCs measured in triplicates from 4 independent experiments (12 h, 3 d, 6 d). **F**, OCN (osteocalcin) level in EDTA-solubilized ECM samples (mean±SD) assessed by ELISA from 4 independent experiments. *P* values were calculated using 1-way ANOVA followed by Dunnett post hoc analysis in **A** and **B** and Student *t* test in **D**, **E**, and **F**. *$P<0.05$, **$P<0.01$, ***$P<0.005$, ****$P<0.001$ when compared with control cells under normoxia.

The Involvement of ROS in Hypoxia-Mediated HIF-1α Upregulation, Osteochondrogenic Differentiation, and ECM Calcification of VSMCs

There is a complex interplay between ROS production and hypoxia in which hypoxia increases ROS production, and excess ROS production increases HIF-1α expression. Therefore, next we examined the role of this interplay between ROS and HIF-1 in the hypoxia-driven osteochondrogenic differentiation and ECM calcification of VSMCs.

To see whether hypoxia influences intracellular ROS production VSMCs were kept under normoxia (21% O_2, 4 hours) or hypoxia (5% O_2, 4 hours) followed by monitoring of ROS
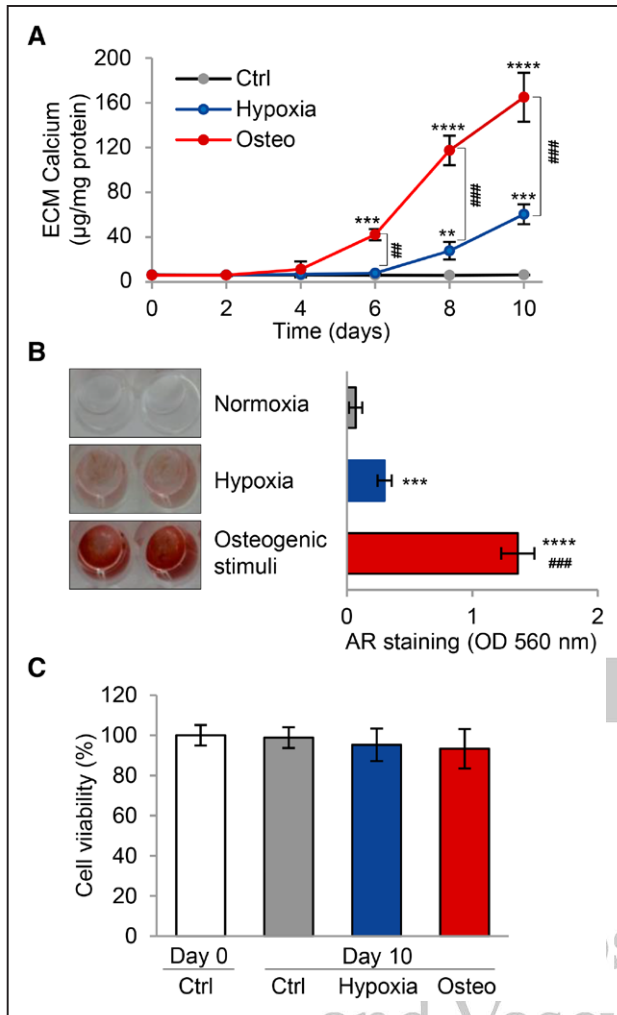
Figure 2. Hypoxia induces extracellular matrix (ECM) calcification of vascular smooth muscle cells (VSMCs). Confluent VSMCs (passage 5–8) were maintained under normoxic (21% O$_2$) or hypoxic (5% O$_2$) conditions or exposed to osteogenic medium (supplemented with 2.5 mmol/L phosphate, 0.6 mmol/L Ca) for 10 days. **A**, Time course of Ca accumulation in ECM (mean±SD). Data derived from 3 independent experiments performed in triplicates. **B**, Representative alizarin red staining (day 10) and quantification (mean±SD) of 3 independent experiments performed in duplicates (optical density [OD]). **C**, Cell viability determined after 10 days of treatment. Mean±SD from 3 independent experiments performed in quadruplicates is shown. *P* values were calculated using 1-way ANOVA followed by Tukey multiple comparison analysis. **P<0.01, ***P<0.005, ****P<0.001 when compared with control cells under normoxia, ##*P*<0.01, ###*P*<0.005 in comparison between hypoxic and osteogenic conditions.

production over an additional 4-hour period. Compared with normoxic condition, hypoxia increased ROS production in VSMCs (Figure 4A). Hypoxia-driven elevation of ROS production was abrogated by the broad ROS scavenger NAC (5 mmol/L) and the H$_2$O$_2$ scavenger SP (5 mmol/L; Figure 4B). In contrast, the superoxide dismutase mimetic manganese (III) tetrakis (4-benzoic acid) porphyrin chloride (50 µmol/L) failed to inhibit hypoxia-mediated ROS production (Figure 4B). To investigate the source of ROS production under hypoxia we applied NADPH oxidase 1/4 inhibitor (GKT137831, GKT, 20 µmol/L) and rotenone (5 µmol/L) that inhibits mitochondrial ROS formation. Rotenone reduced, whereas GKT had no effect on hypoxia-induced ROS production (Figure 4C). Then

we tested the effect of NAC, SP, and rotenone on hypoxia-induced upregulation of HIF-1α. All the 3 ROS scavengers inhibited hypoxia-induced elevation of HIF-1α expression (12 hours; Figure 4D). These results suggested that ROS, and particularly H$_2$O$_2$, plays a role in hypoxia-driven increase in HIF-1α expression. To further confirm the involvement of H$_2$O$_2$ in the upregulation of HIF-1α, next we treated VSMCs with H$_2$O$_2$ (1, 10, 100 µmol/L, 30 minutes) and evaluated protein expression of HIF-1α. We found that H$_2$O$_2$ markedly induced the expression of HIF-1α in VSMCs (Figure 4E). Then, to address whether HIF-1 activation is required for hypoxia-driven ROS production, we measured ROS production in VSMCs exposed to hypoxia (5%, 4 hours) in the presence or absence of chetomin (6 nmol/L). Chetomin completely abolished hypoxia-mediated ROS formation (Figure 4F), suggesting that HIF-1 activation is involved in hypoxia-driven ROS production in VSMCs.

Following this we investigated whether inhibition of ROS formation influences hypoxia-driven osteochondrogenic differentiation and ECM calcification of VSMCs. We found that the ROS inhibitors NAC, SP, and rotenone attenuated hypoxia-mediated increases in mRNA levels of osteochondrogenic transcription factors, that is, *RUNX2* and *SOX9* (6 hours) and diminished the hypoxia-driven upregulation of RUNX2 protein expression (12 hours; Figure 5A through 5C). In addition, we found that NAC, SP, and rotenone inhibited hypoxia-induced ECM calcification assessed by alizarin red staining (Figure 5D, day 10). Furthermore, calcium (day 10) and OCN (day 15) levels of ECM of hypoxia-treated VSMCs were largely attenuated by NAC, SP, and rotenone (Figure 5E and 5F). These results pointed out a fundamental role of excess ROS formation in HIF-1α upregulation as well as in the process of VSMC osteochondrogenic differentiation and subsequent calcification under hypoxic conditions.

Hypoxia Induces Upregulation of RUNX2 in Mice Lung and Aorta In Vivo and Induces Calcification of Mice Aorta Ex Vivo

To investigate whether hypoxia induces osteochondrogenic reprogramming in vivo, we exposed C57BL/6 mice to hypoxia (10% O$_2$) for 12, 24, and 48 hours. Lungs and aortas were harvested for analysis from hypoxia-exposed and control (21% O$_2$) mice. As expected, hypoxia triggered upregulation of Glut-1 at 12 hours in the lung (Figure 6A). In addition, 24-hour hypoxia exposure induced a 1.7-fold increase in RUNX2 mRNA expression in the lung (Figure 6B). Similarly to that of lung, Glut-1 mRNA was elevated in the aorta of hypoxia-treated mice at 12-hour time point (Figure 6C). We found persistent elevation (≈2- to 3-fold) of RUNX2 mRNA expression in the aorta at all time points compared with normoxia controls (Figure 6D).

Recently, a novel organ culture model of aorta has been established to study VC.[39] We used this approach to assess the effect of hypoxia on VC. We dissected aortas from C57BL/6 mice and cultured under normoxic or hypoxic conditions. As positive control, we used osteogenic medium, supplemented with 2.5 mmol/L phosphate. After 6 days of culture, we determined Ca content of the aortas. Osteogenic medium triggered
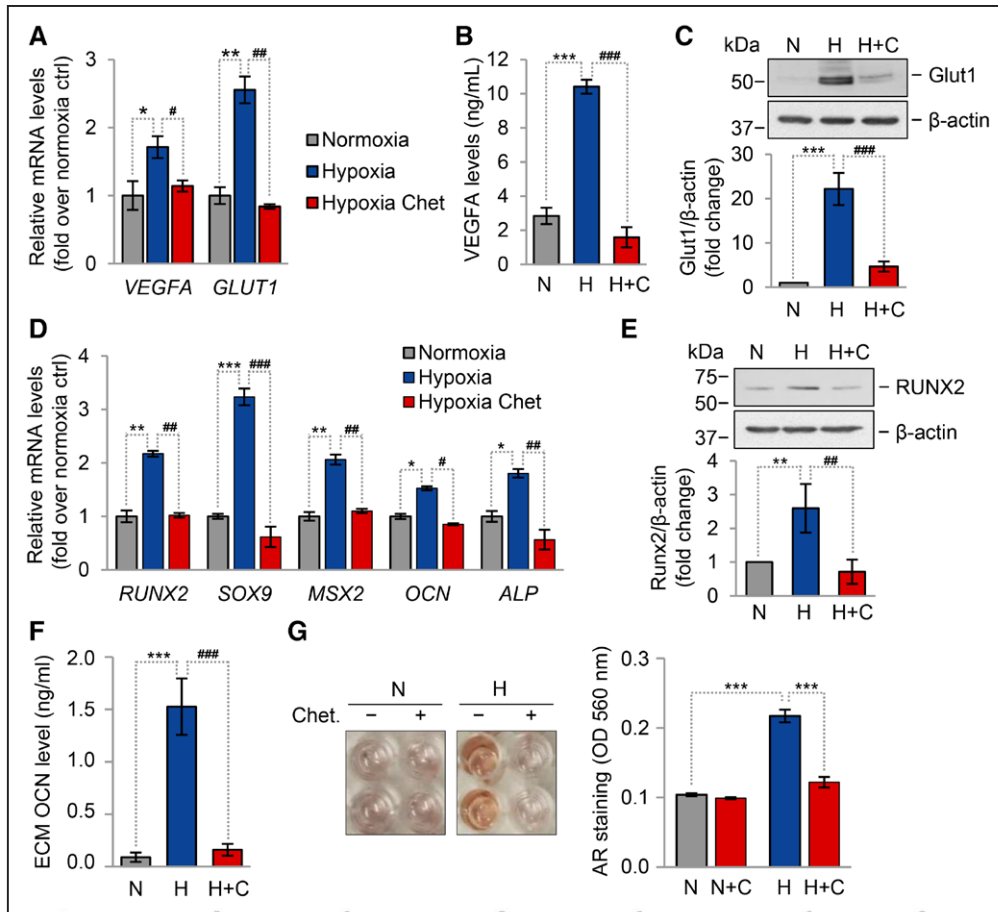
Figure 3. Hypoxia triggers osteochondrogenic differentiation of vascular smooth muscle cells (VSMCs) through HIF (hypoxia-inducible factor)-1. Confluent VSMCs (passage 5–8) were maintained under normoxic (N, 21% O_2) or hypoxic (H, 5% O_2) conditions in the presence or absence of the HIF-1 inhibitor chetomin (Chet/C, 6 nmol/L). **A**, Relative mRNA expressions (6 h, mean±SD) of VEGFA (vascular endothelial growth factor A) and GLUT1 (glucose transporter 1) normalized to GAPDH from 3 independent experiments performed in triplicates. **B**, VEGFA levels (48 h, mean±SD) were determined from cellular supernatant by ELISA in triplicates from 3 independent experiments. **C**, Glut-1 and β-actin protein expressions detected by Western Blot from whole cell lysate (12 h). Representative Western blots from 3 independent experiments. Densitometry analysis (mean±SD) of 3 independent experiments. **D**, Relative mRNA expressions (6 h, mean±SD) of RUNX2 (runt-related transcription factor 2), SOX9 (Sry-related HMG box-9), MSX2 (Msh Homeobox 2), OCN (osteocalcin), and ALP (alkaline phosphatase) normalized to GAPDH from 3 independent experiments performed in triplicates. **E**, RUNX2 and β-actin protein expressions detected by Western Blot from whole cell lysate (12 h). Representative Western blots from 3 independent experiments. Densitometry analysis (mean±SD) of 3 independent experiments. **F**, OCN protein in EDTA-solubilized ECM samples (day 15, mean±SD) measured by ELISA in triplicates from 3 independent experiments. **G**, Representative alizarin red staining (day 10) and quantification (mean±SD) of 3 independent experiments performed in duplicates (optical density [OD]). *P* values were calculated using 1-way ANOVA followed by Tukey multiple comparison analysis. *$P<0.05$, **$P<0.01$, ***$P<0.005$ when compared with control cells under normoxia, #$P<0.05$, ##$P<0.01$, ###$P<0.005$ in comparison of hypoxia vs hypoxia+chetomin groups.

a 7.6-fold increase in the Ca content of the cultured aortas when compared with control aortas. Importantly, we observed a 5.2-fold elevation in the Ca content of aortas cultured under hypoxic conditions when compared with normoxia controls (Figure 6E). We provided evidence that hypoxia-mediated elevation of ROS production and HIF-1 transcriptional activity are required for hypoxia-mediated osteogenic differentiation of VSMCs in vitro, therefore then we addressed whether ROS and HIF-1 activation plays a role in hypoxia-mediated aorta calcification ex vivo. Our results revealed that the ROS inhibitor NAC (5 mmol/L) as well as chetomin (6 nmol/L) attenuated hypoxia-mediated aorta calcification ex vivo (Figure 6F).

Discussion

For decades, cardiovascular calcification was considered as a passive degenerative process in which calcium and phosphate accumulates in the form of hydroxyapatite in different places

of the cardiovascular system. By now this paradigm changed and it became broadly accepted that cardiovascular calcification is a highly regulated process sharing many features with embryonic bone formation.[40] Osteochondrogenic differentiation of certain cells in the cardiovascular system is considered to be the major cellular mechanism of VC.[14,41,42] Numerous inducers and inhibitors of such osteochondrogenic differentiation have been identified to date.[43]

VC was observed in various diseases associated with systemic or local hypoxia. For example, examination of postmortem lungs in a case-control study revealed that bronchial artery calcification occurs in patients with asthma, and the extent of calcification was related to the duration of the disease.[6] Accelerated coronary artery calcification was observed in patients with chronic obstructive pulmonary disease as well, that was strongly correlated with low arterial blood oxygenation.[7,44] VC is a characteristic feature of atherosclerosis,[45] and
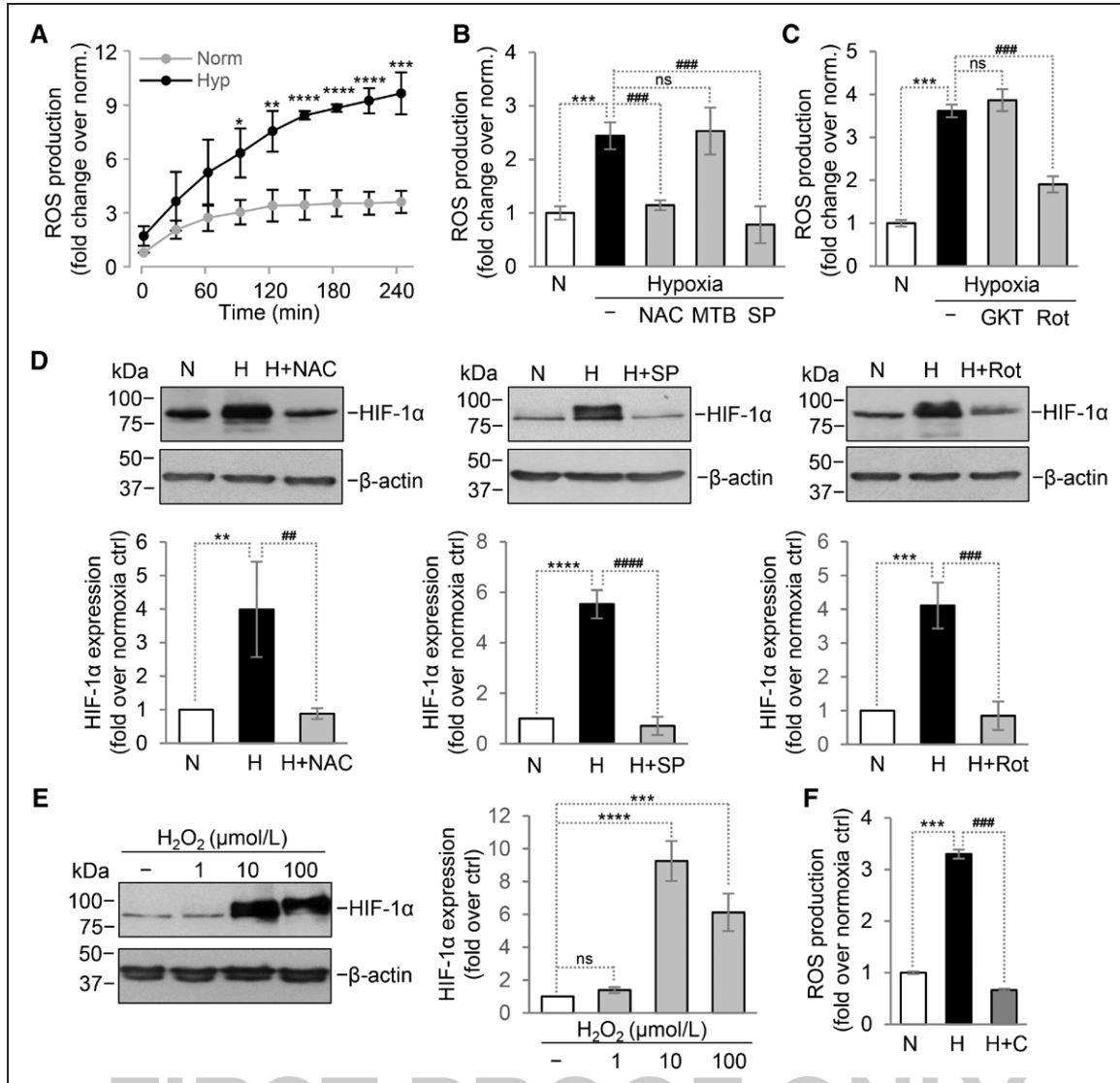
Figure 4. Interplay between reactive oxygen species (ROS) production, HIF (hypoxia-inducible factor)-1α stabilization and HIF-1 activity. **A–D**, Confluent vascular smooth muscle cells (VSMCs) (passage 5–8) were exposed to hypoxia (H, 5% O_2) in the presence or absence of different ROS scavengers; *N*-acetyl cysteine (NAC; 5 mmol/L), Mn(III)-tetrakis (4-benzoic acid) porphyrin chloride (MnTBAP; MTB, 50 μmol/L), sodium pyruvate (SP, 5 mmol/L), GKT (20 μmol/L), and rotenone (Rot, 5 μmol/L). **A**, Intracellular ROS production in VSMCs after a 4-hour exposure to normoxia or hypoxia. ROS was monitored for 4 h following the exposure. Fold change over normoxia at 0 min is shown as mean±SD from 3 independent experiments. **B**, **C**, ROS production of VSMCs exposed to hypoxia (4 h) in the presence of NAC, MTB, SP, GKT, and Rot in comparison to normoxia control. ROS production (mean±SD, 3 h post-treatment) of 3 independent experiments is shown. **D**, HIF-1α and β-actin protein expressions detected by Western Blot from whole cell lysate (12 h). Representative Western blots from 3 independent experiments. Densitometry analysis (mean±SD) of 3 independent experiments. **E**, HIF-1α and β-actin protein expressions detected by Western Blot from whole cell lysate of VSMCs (passage 7–8) exposed to H_2O_2 (30 min, 1–100 μmol/L). **F**, ROS production of VSMCs exposed to hypoxia (4 h) in the presence of chetomin (C, 6 nmol/L) in comparison to normoxia control. ROS production (mean±SD, 3 h post-treatment) of 3 independent experiments is shown. *P* values were calculated using Student *t* test in **A** 1-way ANOVA followed by Tukey multiple comparison analysis in **B–D** and **F** or Dunnett post hoc analysis in **E**. *$P<0.05$, **$P<0.01$, ***$P<0.005$, ****$P<0.001$ when compared with control cells under normoxia. ##$P<0.01$, ###$P<0.005$ in comparison of hypoxia vs hypoxia+inhibitor groups.

intimal spotty calcification frequently associates with intra-plaque neovascularization, a hallmark of plaque hypoxia.[46] Plaque hypoxia contributes to atheroma evolution, remodeling and vulnerabilization through diverse mechanisms but the question whether hypoxia is directly linked to atherosclerotic plaque calcification has not been addressed.[47–50]

Because hypoxia is a common denominator in diseases associated with VC here we investigated whether hypoxia per se triggers osteochondrogenic differentiation of VSMCs. Our study provides evidence that hypoxia induces osteochondrogenic reprogramming and subsequent ECM calcification of VSMCs. We describe the critical role of HIF-1 activation and ROS in the osteochondrogenic effect of hypoxia.

Different cells of the cardiovascular system can undergo osteochondrogenic differentiation.[14,41,42] Here, we focused on human aortic VSMCs, because it is the most extensively studied in vitro model of VC, and osteochondrogenic differentiation of these cells is critically involved in arterial calcification. We found that hypoxia induced stabilization of HIF-1α and elevated the expressions of hypoxia response genes, VEGFA and
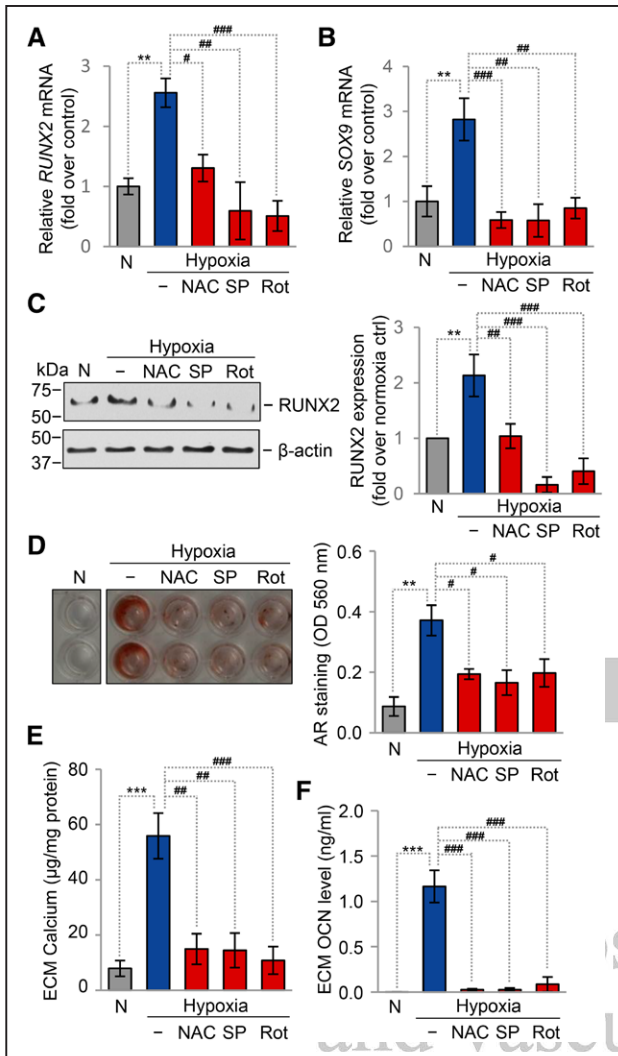
Figure 5. Reactive oxygen species (ROS) are involved in hypoxia-mediated osteochondrogenic differentiation and extracellular matrix (ECM) calcification of vascular smooth muscle cells (VSMCs). Confluent VSMCs (passage 5–8) were exposed to hypoxia (H, 5% O_2) in the presence or absence of different ROS scavengers; N-acetyl cysteine (NAC; 5 mmol/L), sodium pyruvate (SP, 5 mmol/L), and rotenone (Rot, 5 μmol/L). **A**, **B**, Relative mRNA expressions (6 h, mean±SD) of RUNX2 (runt-related transcription factor 2) and SOX9 (Sry-related HMG box-9) normalized to GAPDH from 3 independent experiments performed in triplicates. **C**, RUNX2 and β-actin protein expressions detected by Western Blot from whole cell lysate (12 h). Representative Western blots from 3 independent experiments. Densitometry analysis (mean±SD) of 3 independent experiments. **D**, Representative alizarin red staining (day 10) and quantification (mean±SD) of 3 independent experiments performed in duplicates (optical density [OD]). **E**, Ca level of HCl-solubilized ECM samples (day 10, mean±SD) from 3 independent experiments. **F**, OCN (osteocalcin) level in EDTA-solubilized ECM samples (day 15, mean±SD) assessed by ELISA from 3 independent experiments. P values were calculated using 1-way ANOVA followed by Tukey multiple comparison analysis. **$P<0.01$, ***$P<0.005$ when compared with control cells under normoxia. #$P<0.05$, ##$P<0.01$, ###$P<0.005$ in comparison of hypoxia vs hypoxia+inhibitor groups.

Figure 6. Hypoxia induces osteochondrogenic reprogramming in mice lung and aorta. **A–D**, C57BL/6 mice were exposed to hypoxia (10% O_2) for 12, 24, or 48 h (N=6, each time points). Control mice were exposed to normoxia (N=6). Relative mRNA expressions (mean±SD) of GLUT1 (glucose transporter 1) and RUNX2 (runt-related transcription factor 2) normalized to cyclophilin A in lung and aorta. **E**, **F**, Cleaned whole aortas from C57BL/6 mice were cultured ex vivo under normoxic (N, n=5), hypoxic (Hyp, n=5), and osteogenic (Osteo, n=5) conditions for 6 days. In a separate experiment aortas were cultured under hypoxic conditions in the presence of N-acetyl cysteine (NAC; 5 mmol/L) or chetomin (Chet; 6 nmol/L; n=5 per group). Ca content of aortas normalized to wet aorta weight (mean±SD). P values were calculated using 1-way ANOVA followed by Dunnett post hoc analysis in **A–E** and Tukey multiple comparison analysis in **F**. *$P<0.05$, **$P<0.01$, ***$P<0.005$ when compared with normoxia controls. ##$P<0.01$ in comparison of hypoxia vs hypoxia+inhibitor groups.

GLUT1 in VSMCs. Besides this response, hypoxia triggered an osteochondrogenic differentiation program characterized by upregulation of osteochondrogenic transcription factors and bone-specific proteins in VSMCs. Hypoxia-mediated switch of the osteochondrogenic reprogramming in VSMCs eventually led to elevated ECM calcification in vitro.
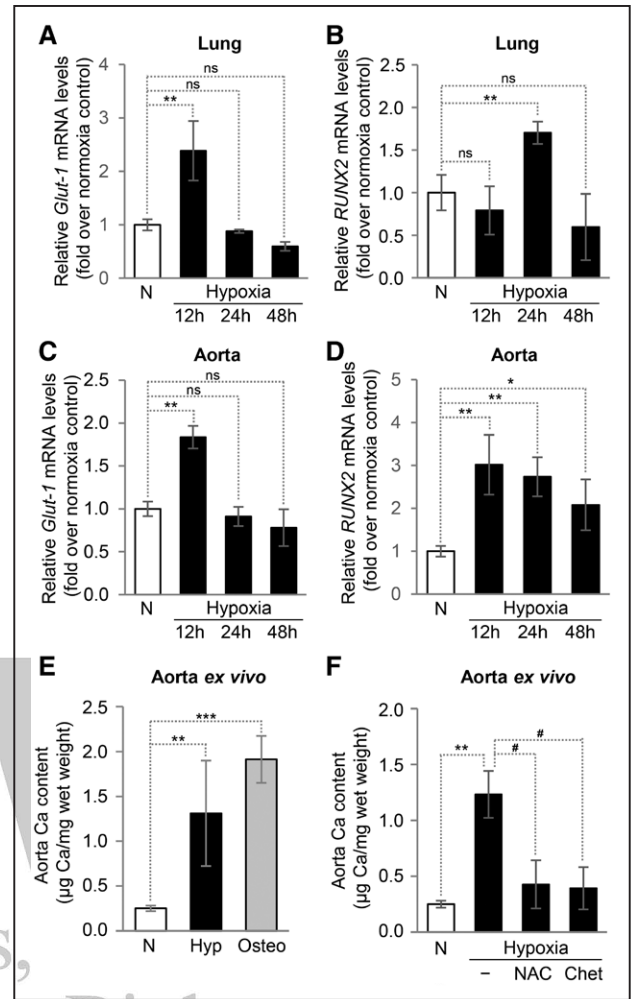
The effect of hypoxia on osteogenic capability was studied previously in diverse osseous and pluripotent mesenchymal cells. Park et al[51] showed that hypoxia (2% O_2) decreases the expressions of RUNX2, OCN, and ALP in MG63 osteoblast-like cells. In contrast, Salim et al[52] found that hypoxia (2% O_2) had little effect on osteogenic differentiation of primary osteoblasts and mesenchymal precursors, but short-term anoxic treatment inhibited in vitro bone nodule formation and calcium deposition in both cell types through downregulation of RUNX2. On the contrary Wagegg et al[53] reported that hypoxia promotes osteogenesis of multipotent human mesenchymal stromal cells in an HIF-1 and RUNX2-dependent way. Ichijima et al[54] showed that hypoxia

induced osteogenesis of periosteal cells. Regarding smooth muscle cells, Mokas et al[21] showed that hypoxia enhances phosphate-mediated osteogenic differentiation and calcification of VSMCs.

These results suggest that hypoxia regulates osteogenic differentiation in a highly sensitive and a cell-specific manner. Considering that RUNX2 is the master regulator of osteogenic differentiation, the high variability of the hypoxia responses described in diverse cells could be at least partially explained by the differences in RUNX2 promoter activity in osseous and nonosseous cells.[55]

Cellular and systemic homeostatic response to hypoxia is regulated by the HIF-1 pathway. HIF-1 is a heterodimer basic helix-loop-helix-PAS domain transcription factor, composed of an oxygen-sensitive α subunit (HIF-1α) and a stable β subunit.[18] Under normoxia, HIF-1α is constantly synthesized and degraded, while under hypoxia, HIF-1α is stable and dimerizes with the β subunit.[18] The heterodimer translocate into the nucleus, binds to cis-acting hypoxia response elements in HIF-1 target genes, recruits coactivator molecules, that is, p300 and CREB-binding protein, and the complex activates transcription.[18] Here we showed that inhibition of the HIF-1 pathway abolished hypoxia-mediated osteochondrogenic differentiation of VSMCs, suggesting that HIF-1 activation is critically involved in the osteochondrogenic effect of hypoxia. Our results are in strong agreement with the work of Ruffenach et al[22] in which they showed that overexpression of HIF-1α promotes, whereas adenovirus expressing a dominant negative form of HIF-1α inhibits calcification of pulmonary artery smooth muscle cells. These findings are also supported by the previous clinical observation that HIF-1α plasma levels significantly and independently predict the presence of coronary artery calcification in patients with type 2 diabetes mellitus.[19]

Recent evidence suggests a complex interplay between HIF-1 and RUNX2 in the regulation of osteogenic differentiation. Our results revealed that hypoxia induces the expression of RUNX2, which effect was dependent on HIF-1 activity. On the other hand Mokas et al[21] showed that induction of RUNX2 by elevated phosphate leads to HIF-1α stabilization. In addition, Ruffenach et al[22] showed that overexpression of RUNX2 triggers HIF-1α activation. In the recent years, regulation of RUNX2 through the epigenetic reader BRD4 (bromodomain protein 4) has been established. BRD4 induces RUNX2 transcription in cancer cells.[56] BRD4 expression is elevated in lungs, distal pulmonary arteries, pulmonary artery smooth muscle cells, and coronary arteries of patient with pulmonary arterial hypertension, that contributes to vascular remodeling and the development of coronary artery disease.[57,58] Inhibition of BRD4 has been shown to reverse hypoxia-induced pulmonary arterial hypertension[57] and suppress VC in a hypercholesterolemic mice model.[59]

Although it sounds paradoxical, hypoxia stimulates ROS production in diverse mammalian cells.[60] Studies showed that mitochondrial electron transport chain complexes I and III and NADPH oxidases are involved in hypoxia-mediated increase in ROS production.[60–63] Moreover, the finding that mitochondria-targeted antioxidants abolish the hypoxia response proved that mitochondrial ROS production is essential

for propagation of the hypoxic signal toward the activation of the HIF pathway.[64]

Based on this evidence we hypothesized that hypoxia-mediated elevation of mitochondrial ROS production could critically participate in hypoxia-mediated osteochondrogenic differentiation of VSMCs. In line of this notion here we confirmed that hypoxia triggers elevated ROS production in VSMCs. Inhibition of ROS production with NAC and the mitochondrial complex I inhibitor rotenone abolished hypoxia-induced HIF-1α stabilization and inhibited hypoxia-induced upregulations of RUNX2, SOX9, and OCN and attenuated calcification.

Previous studies already suggested a causative role of excessive ROS production in cardiovascular pathophysiology including VC.[32–34] Osteogenic differentiation of VSMCs has been linked to enhanced ROS production, and vascular cells expressing osteogenic markers were identified as sources of excess ROS around calcifying foci.[33] Importantly, Zhao et al[34] showed that inhibition of mitochondrial ROS generation attenuates phosphate-mediated osteogenic differentiation of VSMCs. Byon et al[65] showed that hydrogen peroxide promotes osteogenic differentiation of VSMCs through the induction of RUNX2. In agreement with these findings here we showed that hypoxia-mediated production of hydrogen peroxide plays an essential role in the stabilization of HIF-1α and in the promotion of osteochondrogenic response in VSMCs. We found that hydrogen peroxide is sufficient to stabilize HIF-1α under normoxic condition in VSMCs which is in agreement with previous observations.[28,66]

Inhibition of HIF-1 stabilization by ROS scavengers under hypoxic conditions suggests that ROS generation is upstream of HIF-1 stabilization in VSMCs under hypoxia, as has been described in many other experimental conditions and recognized as hypoxia/ROS/HIF-1 axis.[31,67]

Interestingly, we also found that inhibition of HIF-1 activity abolished hypoxia-mediated ROS production, suggesting a more complex interplay between ROS generation and HIF-1 activity. A similar phenomenon was described in a previous study, in which decreased ROS production was observed in heterozygous HIF-1α deficient mice upon hypoxia exposure.[68] The authors suggested that once HIF-1 is activated, it may function to maintain increased ROS levels and they proposed a positive feed-forward loop between ROS and HIF-1 activity.[68] This might be implicated in our experimental settings, which needs to be further investigated.

Hypoxia and accelerated arterial calcification coincide in diverse diseases such as asthma, chronic obstructive pulmonary disease, and obstructive sleep apnea.[6–8] Here we showed that hypoxia upregulates RUNX2 expression in mice lung and aorta in vivo. In addition, using an ex vivo organ culture approach we showed that hypoxia triggers Ca accumulation in mouse aorta in an HIF-1–dependent and ROS-dependent manner.

To conclude, data reported in the present study suggest that hypoxia is an independent factor sufficient to trigger osteochondrogenic differentiation of VSMCs. We propose that unfettered generation of ROS during hypoxia may be the signal switching on the osteochondrogenic differentiation program of VSMCs that leads eventually to VC.

References

1. Rennenberg RJ, Kessels AG, Schurgers LJ, van Engelshoven JM, de Leeuw PW, Kroon AA. Vascular calcifications as a marker of increased cardiovascular risk: a meta-analysis. *Vasc Health Risk Manag.* 2009;5:185–197.

2. Wilson PW, Kauppila LI, O'Donnell CJ, Kiel DP, Hannan M, Polak JM, Cupples LA. Abdominal aortic calcific deposits are an important predictor of vascular morbidity and mortality. *Circulation.* 2001;103:1529–1534.

3. McClelland RL, Chung H, Detrano R, Post W, Kronmal RA. Distribution of coronary artery calcium by race, gender, and age: results from the Multi-Ethnic Study of Atherosclerosis (MESA). *Circulation.* 2006;113:30–37. doi: 10.1161/CIRCULATIONAHA.105.580696

4. Leopold JA. Vascular calcification: an age-old problem of old age. *Circulation.* 2013;127:2380–2382. doi: 10.1161/CIRCULATIONAHA.113.003341

5. Virmani R, Joner M, Sakakura K. Recent highlights of ATVB: calcification. *Arterioscler Thromb Vasc Biol.* 2014;34:1329–1332. doi: 10.1161/ATVBAHA.114.304000

6. Green FH, Butt JC, James AL, Carroll NG. Abnormalities of the bronchial arteries in asthma. *Chest.* 2006;130:1025–1033. doi: 10.1378/chest.130.4.1025

7. Williams MC, Murchison JT, Edwards LD, et al.; Evaluation of COPD Longitudinally to Identify Predictive Surrogate Endpoints (ECLIPSE) investigators. Coronary artery calcification is increased in patients with COPD and associated with increased morbidity and mortality. *Thorax.* 2014;69:718–723. doi: 10.1136/thoraxjnl-2012-203151

8. Tachikawa R, Koyasu S, Matsumoto T, Hamada S, Azuma M, Murase K, Tanizawa K, Inouchi M, Oga T, Mishima M, Togashi K, Chin K. Obstructive sleep apnea and abdominal aortic calcification: Is there an association independent of comorbid risk factors? *Atherosclerosis.* 2015;241:6–11. doi: 10.1016/j.atherosclerosis.2015.04.801

9. Steitz SA, Speer MY, Curinga G, Yang HY, Haynes P, Aebersold R, Schinke T, Karsenty G, Giachelli CM. Smooth muscle cell phenotypic transition associated with calcification: upregulation of Cbfa1 and downregulation of smooth muscle lineage markers. *Circ Res.* 2001;89:1147–1154.

10. Shroff R, Long DA, Shanahan C. Mechanistic insights into vascular calcification in CKD. *J Am Soc Nephrol.* 2013;24:179–189. doi: 10.1681/ASN.2011121191

11. Mori K, Shioi A, Jono S, Nishizawa Y, Morii H. Dexamethasone enhances *In vitro* vascular calcification by promoting osteoblastic differentiation of vascular smooth muscle cells. *Arterioscler Thromb Vasc Biol.* 1999;19:2112–2118.

12. Tyson KL, Reynolds JL, McNair R, Zhang Q, Weissberg PL, Shanahan CM. Osteo/chondrocytic transcription factors and their target genes exhibit distinct patterns of expression in human arterial calcification. *Arterioscler Thromb Vasc Biol.* 2003;23:489–494. doi: 10.1161/01.ATV.0000059406.92165.31

13. Neven E, Dauwe S, De Broe ME, D'Haese PC, Persy V. Endochondral bone formation is involved in media calcification in rats and in men. *Kidney Int.* 2007;72:574–581. doi: 10.1038/sj.ki.5002353

14. Boström K, Watson KE, Horn S, Wortham C, Herman IM, Demer LL. Bone morphogenetic protein expression in human atherosclerotic lesions. *J Clin Invest.* 1993;91:1800–1809. doi: 10.1172/JCI116391

15. Johnson RC, Leopold JA, Loscalzo J. Vascular calcification: pathobiological mechanisms and clinical implications. *Circ Res.* 2006;99:1044–1059. doi: 10.1161/01.RES.0000249379.55535.21

16. Giachelli CM. Inducers and inhibitors of biomineralization: lessons from pathological calcification. *Orthod Craniofac Res.* 2005;8:229–231. doi: 10.1111/j.1601-6343.2005.00345.x

17. Shroff RC, Shanahan CM. The vascular biology of calcification. *Semin Dial.* 2007;20:103–109. doi: 10.1111/j.1525-139X.2007.00255.x

18. Semenza GL. Hypoxia-inducible factor 1 (HIF-1) pathway. *Sci Stke.* 2007;2007:cm8. doi: 10.1126/stke.4072007cm8

19. Li G, Lu WH, Ai R, Yang JH, Chen F, Tang ZZ. The relationship between serum hypoxia-inducible factor 1α and coronary artery calcification in asymptomatic type 2 diabetic patients. *Cardiovasc Diabetol.* 2014;13:52. doi: 10.1186/1475-2840-13-52

20. Perrotta I, Moraca FM, Sciangula A, Aquila S, Mazzulla S. HIF-1α and VEGF: immunohistochemical profile and possible function in human aortic valve stenosis. *Ultrastruct Pathol.* 2015;39:198–206. doi: 10.3109/01913123.2014.991884

21. Mokas S, Larivière R, Lamalice L, Gobeil S, Cornfield DN, Agharazii M, Richard DE. Hypoxia-inducible factor-1 plays a role in phosphate-induced vascular smooth muscle cell calcification. *Kidney Int.* 2016;90:598–609. doi: 10.1016/j.kint.2016.05.020

22. Ruffenach G, Chabot S, Tanguay VF, et al. Role for runt-related transcription factor 2 in proliferative and calcified vascular lesions in pulmonary arterial hypertension. *Am J Respir Crit Care Med.* 2016;194:1273–1285. doi: 10.1164/rccm.201512-2380OC

23. Fuhrmann DC, Brüne B. Mitochondrial composition and function under the control of hypoxia. *Redox Biol.* 2017;12:208–215. doi: 10.1016/j.redox.2017.02.012

24. Papandreou I, Cairns RA, Fontana L, Lim AL, Denko NC. HIF-1 mediates adaptation to hypoxia by actively downregulating mitochondrial oxygen consumption. *Cell Metab.* 2006;3:187–197. doi: 10.1016/j.cmet.2006.01.012

25. Cash TP, Pan Y, Simon MC. Reactive oxygen species and cellular oxygen sensing. *Free Radic Biol Med.* 2007;43:1219–1225. doi: 10.1016/j.freeradbiomed.2007.07.001

26. Paddenberg R, Ishaq B, Goldenberg A, Faulhammer P, Rose F, Weissmann N, Braun-Dullaeus RC, Kummer W. Essential role of complex II of the respiratory chain in hypoxia-induced ROS generation in the pulmonary vasculature. *Am J Physiol Lung Cell Mol Physiol.* 2003;284:L710–L719. doi: 10.1152/ajplung.00149.2002

27. Chandel NS, McClintock DS, Feliciano CE, Wood TM, Melendez JA, Rodriguez AM, Schumacker PT. Reactive oxygen species generated at mitochondrial complex III stabilize hypoxia-inducible factor-1alpha during hypoxia: a mechanism of O2 sensing. *J Biol Chem.* 2000;275:25130–25138. doi: 10.1074/jbc.M001914200

28. Hamanaka RB, Chandel NS. Mitochondrial reactive oxygen species regulate hypoxic signaling. *Curr Opin Cell Biol.* 2009;21:894–899. doi: 10.1016/j.ceb.2009.08.005

29. Waypa GB, Smith KA, Schumacker PT. O2 sensing, mitochondria and ROS signaling: the fog is lifting. *Mol Aspects Med.* 2016;47–48:76–89. doi: 10.1016/j.mam.2016.01.002

30. Sato H, Sato M, Kanai H, Uchiyama T, Iso T, Ohyama Y, Sakamoto H, Tamura J, Nagai R, Kurabayashi M. Mitochondrial reactive oxygen species and c-Src play a critical role in hypoxic response in vascular smooth muscle cells. *Cardiovasc Res.* 2005;67:714–722. doi: 10.1016/j.cardiores.2005.04.017

31. Hielscher A, Gerecht S. Hypoxia and free radicals: role in tumor progression and the use of engineering-based platforms to address these relationships. *Free Radic Biol Med.* 2015;79:281–291. doi: 10.1016/j.freeradbiomed.2014.09.015

32. Byon CH, Heath JM, Chen Y. Redox signaling in cardiovascular pathophysiology: a focus on hydrogen peroxide and vascular smooth muscle cells. *Redox Biol.* 2016;9:244–253. doi: 10.1016/j.redox.2016.08.015

33. Liberman M, Bassi E, Martinatti MK, Lario FC, Wosniak J Jr, Pomerantzeff PM, Laurindo FR. Oxidant generation predominates around calcifying foci and enhances progression of aortic valve calcification. *Arterioscler Thromb Vasc Biol.* 2008;28:463–470. doi: 10.1161/ATVBAHA.107.156745

34. Zhao MM, Xu MJ, Cai Y, Zhao G, Guan Y, Kong W, Tang C, Wang X. Mitochondrial reactive oxygen species promote p65 nuclear translocation mediating high-phosphate-induced vascular calcification in vitro and in vivo. *Kidney Int.* 2011;79:1071–1079. doi: 10.1038/ki.2011.18

35. Balogh E, Tóth A, Tolnai E, Bodó T, Bányai E, Szabó DJ, Petrovski G, Jeney V. Osteogenic differentiation of human lens epithelial cells might contribute to lens calcification. *Biochim Biophys Acta.* 2016;1862:1724–1731. doi: 10.1016/j.bbadis.2016.06.012

36. Jeney V, Balla J, Yachie A, Varga Z, Vercellotti GM, Eaton JW, Balla G. Pro-oxidant and cytotoxic effects of circulating heme. *Blood.* 2002;100:879–887.

37. Zarjou A, Jeney V, Arosio P, Poli M, Zavaczki E, Balla G, Balla J. Ferritin ferroxidase activity: a potent inhibitor of osteogenesis. *J Bone Miner Res.* 2010;25:164–172. doi: 10.1359/jbmr.091002

38. Balogh E, Tolnai E, Nagy B Jr, Nagy B, Balla G, Balla J, Jeney V. Iron overload inhibits osteogenic commitment and differentiation of

mesenchymal stem cells via the induction of ferritin. *Biochim Biophys Acta*. 2016;1862:1640–1649. doi: 10.1016/j.bbadis.2016.06.003

39. Akiyoshi T, Ota H, Iijima K, Son BK, Kahyo T, Setou M, Ogawa S, Ouchi Y, Akishita M. A novel organ culture model of aorta for vascular calcification. *Atherosclerosis*. 2016;244:51–58. doi: 10.1016/j.atherosclerosis.2015.11.005

40. Demer LL, Tintut Y. Vascular calcification: pathobiology of a multi-faceted disease. *Circulation*. 2008;117:2938–2948. doi: 10.1161/CIRCULATIONAHA.107.743161

41. Shioi A, Nishizawa Y, Jono S, Koyama H, Hosoi M, Morii H. Beta-glycerophosphate accelerates calcification in cultured bovine vascular smooth muscle cells. *Arterioscler Thromb Vasc Biol*. 1995;15:2003–2009.

42. Rajamannan NM, Subramaniam M, Rickard D, Stock SR, Donovan J, Springett M, Orszulak T, Fullerton DA, Tajik AJ, Bonow RO, Spelsberg T. Human aortic valve calcification is associated with an osteoblast phenotype. *Circulation*. 2003;107:2181–2184. doi: 10.1161/01.CIR.0000070591.21548.69

43. Lee D. Vascular calcification: Inducers and inhibitors. *Mater Sci Eng B Adv*. 2011;176:1133–1141.

44. Inoue S, Shibata Y, Kishi H, et al. Low arterial blood oxygenation is associated with calcification of the coronary arteries in patients with chronic obstructive pulmonary disease. *Respir Investig*. 2015;53:111–116. doi: 10.1016/j.resinv.2015.01.002

45. Nakahara T, Dweck MR, Narula N, Pisapia D, Narula J, Strauss HW. Coronary artery calcification: from mechanism to molecular imaging. *JACC Cardiovasc Imaging*. 2017;10:582–593. doi: 10.1016/j.jcmg.2017.03.005

46. Ibrahimi P, Jashari F, Nicoll R, Bajraktari G, Wester P, Henein MY. Coronary and carotid atherosclerosis: how useful is the imaging? *Atherosclerosis*. 2013;231:323–333. doi: 10.1016/j.atherosclerosis.2013.09.035

47. Luque A, Turu M, Juan-Babot O, Cardona P, Font A, Carvajal A, Slevin M, Iborra E, Rubio F, Badimon L, Krupinski J. Overexpression of hypoxia/inflammatory markers in atherosclerotic carotid plaques. *Front Biosci*. 2008;13:6483–6490.

48. Deguchi JO, Yamazaki H, Aikawa E, Aikawa M. Chronic hypoxia activates the Akt and beta-catenin pathways in human macrophages. *Arterioscler Thromb Vasc Biol*. 2009;29:1664–1670. doi: 10.1161/ATVBAHA.109.194043

49. Libby P, Folco E. Tension in the plaque: hypoxia modulates metabolism in atheroma. *Circ Res*. 2011;109:1100–1102. doi: 10.1161/RES.0b013e31823bdb84

50. Jeney V, Balla G, Balla J. Red blood cell, hemoglobin and heme in the progression of atherosclerosis. *Front Physiol*. 2014;5:379. doi: 10.3389/fphys.2014.00379

51. Park JH, Park BH, Kim HK, Park TS, Baek HS. Hypoxia decreases Runx2/Cbfa1 expression in human osteoblast-like cells. *Mol Cell Endocrinol*. 2002;192:197–203.

52. Salim A, Nacamuli RP, Morgan EF, Giaccia AJ, Longaker MT. Transient changes in oxygen tension inhibit osteogenic differentiation and Runx2 expression in osteoblasts. *J Biol Chem*. 2004;279:40007–40016. doi: 10.1074/jbc.M403715200

53. Wagegg M, Gaber T, Lohanatha FL, Hahne M, Strehl C, Fangradt M, Tran CL, Schönbeck K, Hoff P, Ode A, Perka C, Duda GN, Buttgereit F. Hypoxia promotes osteogenesis but suppresses adipogenesis of human mesenchymal stromal cells in a hypoxia-inducible factor-1 dependent manner. *PLoS One*. 2012;7:e46483. doi: 10.1371/journal.pone.0046483

54. Ichijima T, Matsuzaka K, Tonogi M, Yamane GY, Inoue T. Osteogenic differences in cultured rat periosteal cells under hypoxic and normal

conditions. *Exp Ther Med*. 2012;3:165–170. doi: 10.3892/etm.2011.393

55. Tamiya H, Ikeda T, Jeong JH, Saito T, Yano F, Jung YK, Ohba S, Kawaguchi H, Chung UI, Choi JY. Analysis of the Runx2 promoter in osseous and non-osseous cells and identification of HIF2A as a potent transcription activator. *Gene*. 2008;416:53–60. doi: 10.1016/j.gene.2008.03.003

56. Lamoureux F, Baud'huin M, Rodriguez Calleja L, Jacques C, Berreur M, Rédini F, Lecanda F, Bradner JE, Heymann D, Ory B. Selective inhibition of BET bromodomain epigenetic signalling interferes with the bone-associated tumour vicious cycle. *Nat Commun*. 2014;5:3511. doi: 10.1038/ncomms4511

57. Meloche J, Potus F, Vaillancourt M, et al. Bromodomain-containing protein 4: the epigenetic origin of pulmonary arterial hypertension. *Circ Res*. 2015;117:525–535. doi: 10.1161/CIRCRESAHA.115.307004

58. Meloche J, Lampron MC, Nadeau V, Maltais M, Potus F, Lambert C, Tremblay E, Vitry G, Breuils-Bonnet S, Boucherat O, Charbonneau E, Provencher S, Paulin R, Bonnet S. Implication of inflammation and epigenetic readers in coronary artery remodeling in patients with pulmonary arterial hypertension. *Arterioscler Thromb Vasc Biol*. 2017;37:1513–1523. doi: 10.1161/ATVBAHA.117.309156

59. Brown JD, Lin CY, Duan Q, et al. NF-κB directs dynamic super enhancer formation in inflammation and atherogenesis. *Mol Cell*. 2014;56:219–231. doi: 10.1016/j.molcel.2014.08.024

60. Smith KA, Waypa GB, Schumacker PT. Redox signaling during hypoxia in mammalian cells. *Redox Biol*. 2017;13:228–234. doi: 10.1016/j.redox.2017.05.020

61. Duranteau J, Chandel NS, Kulisz A, Shao Z, Schumacker PT. Intracellular signaling by reactive oxygen species during hypoxia in cardiomyocytes. *J Biol Chem*. 1998;273:11619–11624.

62. Fernández-Agüera MC, Gao L, González-Rodríguez P, Pintado CO, Arias-Mayenco I, García-Flores P, García-Pergañeda A, Pascual A, Ortega-Sáenz P, López-Barneo J. Oxygen sensing by arterial chemoreceptors depends on mitochondrial complex I signaling. *Cell Metab*. 2015;22:825–837. doi: 10.1016/j.cmet.2015.09.004

63. Ward JP. A twist in the tail: synergism between mitochondria and NADPH oxidase in the hypoxia-induced elevation of reactive oxygen species in pulmonary artery. *Free Radic Biol Med*. 2008;45:1220–1222. doi: 10.1016/j.freeradbiomed.2008.08.015

64. Chandel NS, Maltepe E, Goldwasser E, Mathieu CE, Simon MC, Schumacker PT. Mitochondrial reactive oxygen species trigger hypoxia-induced transcription. *Proc Natl Acad Sci USA*. 1998;95:11715–11720.

65. Byon CH, Javed A, Dai Q, Kappes JC, Clemens TL, Darley-Usmar VM, McDonald JM, Chen Y. Oxidative stress induces vascular calcification through modulation of the osteogenic transcription factor Runx2 by AKT signaling. *J Biol Chem*. 2008;283:15319–15327. doi: 10.1074/jbc.M800021200

66. Richard DE, Berra E, Pouyssegur J. Nonhypoxic pathway mediates the induction of hypoxia-inducible factor 1alpha in vascular smooth muscle cells. *J Biol Chem*. 2000;275:26765–26771. doi: 10.1074/jbc.M003325200

67. Movafagh S, Crook S, Vo K. Regulation of hypoxia-inducible factor-1a by reactive oxygen species: new developments in an old debate. *J Cell Biochem*. 2015;116:696–703. doi: 10.1002/jcb.25074

68. Peng YJ, Yuan G, Ramakrishnan D, Sharma SD, Bosch-Marce M, Kumar GK, Semenza GL, Prabhakar NR. Heterozygous HIF-1alpha deficiency impairs carotid body-mediated systemic responses and reactive oxygen species generation in mice exposed to intermittent hypoxia. *J Physiol*. 2006;577(pt 2):705–716. doi: 10.1113/jphysiol.2006.114033

Highlights

- Hypoxia induces osteochondrogenic differentiation and extracellular matrix calcification in vascular smooth muscle cells.
- HIF-1 (hypoxia-inducible factor 1) activation is involved in hypoxia-mediated osteochondrogenic differentiation and extracellular matrix calcification in vascular smooth muscle cells.
- Hypoxia elevates mitochondrial reactive oxygen species formation in vascular smooth muscle cells, which is indispensable in hypoxia-driven osteochondrogenic differentiation of vascular smooth muscle cells.
- Hypoxia induces osteochondrogenic reprogramming in the mouse aorta.